PAPER

Application of a mode-locked fiber laser for highly time resolved broadband absorption spectroscopy and laser-assisted breakdown on micro-plasmas

To cite this article: B Niermann *et al* 2012 *J. Phys. D: Appl. Phys.* **45** 245202

View the article online for updates and enhancements.

Related content

- Review on VUV to MIR absorption spectroscopy of atmospheric pressure plasma jets
  Stephan Reuter, Joao Santos Sousa, Gabi Daniel Stancu et al.

- Argon metastable dynamics in a filamentary jet micro-discharge at atmospheric pressure
  B Niermann, R Reuter, T Kuschel et al.

- Continuous-wave femtosecond lasers
  P G Kryukov

Recent citations

- Review on VUV to MIR absorption spectroscopy of atmospheric pressure plasma jets
  Stephan Reuter *et al*

- Broadband picosecond radiation source based on noncollinear optical parametric amplifier
  V G Arakcheev *et al*

- Density of atoms in Ar(3p54s) states and gas temperatures in an argon surfatron plasma measured by tunable laser spectroscopy
  S. Hubner *et al*
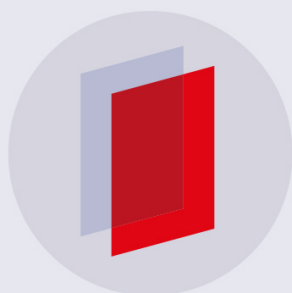
IOP ebooks™

Bringing you innovative digital publishing with leading voices to create your essential collection of books in STEM research.

Start exploring the collection - download the first chapter of every title for free.

Application of a mode-locked fiber laser for highly time resolved broadband absorption spectroscopy and laser-assisted breakdown on micro-plasmas

B Niermann[1], I L Budunoğlu[2], K Gürel[2], M Böke[1] F Ö Ilday[2] and J Winter[1]

[1] Ruhr-University Bochum, Institute for Experimental Physics II, Universitätsstraße 150, 44780 Bochum, Germany

[2] Bilkent University, Ultrafast Optics and Lasers Group, Department of Physics, Cankaya, Ankara 06800, Turkey

E-mail: benedikt.niermann@rub.de

Abstract

Absorption spectroscopy is known to be a powerful tool to gain spatially and temporally resolved information on excited and reactive species in a plasma discharge. Furthermore, the interaction of the discharge with short intense laser pulses can trigger the ignition and the transition into other transient states of the plasma. In this context laser-assisted 'pump-probe' experiments involving simultaneously generated supercontinuum radiation yield highly temporally resolved and spatially well-defined information on the transient phenomena. In this paper we demonstrate the possibility for 'pump–probe' experiments by initiating breakdown on a picosecond time scale ('pump') with a high-power beam and measuring the broadband absorption with the simultaneously provided supercontinuum ('probe'). Since both pulses are generated from the same mode-locked master oscillator, they have a strong level of synchronization.

(Some figures may appear in colour only in the online journal)

1. Introduction

In recent years, research on micro-plasmas has become a strong focus in plasma science [3]. However, due to their operation at atmospheric pressure and transient phenomena occurring at fast time scales, new methods are needed for quantitative and reliable analysis of their various discharge modes. In this paper we discuss and demonstrate the possibility of investigating these transient phenomena by absorption spectroscopy and laser-assisted 'pump-probe' experiments. Key elements in this context are the generation of a broad supercontinuum spectrum, the application of broad-band absorption spectroscopy (BBAS) on micro-plasmas, the ignition of the discharge as well as the transfer of it to different modes by strong laser fields, and finally the

triggering and synchronization of aforementioned points for highly temporally resolved analysis of transient phenomena.

1.1. Absorption spectroscopy

Measuring the optical absorption of plasma species is a powerful method to deduce quantitative information of the (line-integrated) species density using the Lambert–Beer law. Among the most frequently used techniques are BBAS [1], tunable diode laser absorption spectroscopy (TDLAS) [2, 7, 8] and cavity ring-down spectroscopy (CRDS) [1, 23, 24]. The advantage of BBAS over TDLAS is the coverage of a large spectral range facilitating the simultaneous measurement of several species in a plasma absorbing at different wavelengths. Its disadvantage compared with TDLAS is its lower spectral

resolution. On the other hand, essentially for each optical transition a separate diode laser has to be employed for TDLAS. The advantage of CRDS is its very high sensitivity, provided that a long absorption length between two mirrors of very high reflectivity can be realized. In this technique, the characteristic decay time of the intensity of a light pulse is measured, which is coupled into the cavity with the species of interest. Due to the very small plasma volume, CRDS is difficult to realize if spatial resolution is required [11, 24]. Both TDLAS and BBAS have been successfully applied to micro-plasmas [4–6, 8–10]. Absorbances are usually small, rarely exceeding 10^{-3}, requiring in both cases a very stable setup. Often lock-in techniques or other refined optical techniques are used to increase sensitivity. Since in low-pressure plasmas the width of the absorption lines is of the order of a few GHz, a very high resolution spectrometer is required for BBAS, whereas the line width of diode lasers in TDLAS is of the order of MHz and small compared with the absorption lines. This allows a precise measurement of the line profiles and may allow one to deduce, e.g., the gas temperature or the electron density. In atmospheric pressure plasmas, the absorption lines are significantly broadened [8]. On the one hand, this reduces the signal-to-noise ratio further, but it alleviates, however, the line detection in BBAS. The highest signal-to-noise ratio is obtained when the spectral resolution of the spectrograph is identical to the line width [13].

For BBAS, several different light sources may be used such as, incandescent filaments, high-pressure Xe lamps or light-emitting diodes [10, 12, 13]. These light sources have to be well stabilized using precision power supplies and temperature control. They are normally not pulsed and spatially incoherent or at least highly multi-mode. Using a fast external chopper for lock-in techniques is important. Particularly interesting for the investigation of micro-plasmas is the use of supercontinuum radiation [14] generated from coupling very short pulse lasers into a photonic crystal fibre (PCF) [15]. Since this process produces pulses which are still in the picosecond range, typically with sub-picosecond timing jitter values, the use of the supercontinuum pulses allows superb time resolution of the measurement.

1.2. Laser-assisted plasma breakdown

It is well-known that high intensities of laser radiation may induce a breakdown in gases and at surfaces together with the formation of a plasma [16–21]. Several studies on gas breakdown and surface-assisted breakdown have been published and threshold values for breakdown have been communicated [18]. However, the data show a large scatter. It appears that several mechanisms may be invoked: very large electric field strength at high local laser powers, secondary electron emission from the surfaces at low enough wavelength and/or materials ablation/heating with subsequent charge carrier emission. These mechanisms may act simultaneously. It is usually observed that threshold values for gas breakdown increase for a given system with the wavelength of the laser light [18]. Laser irradiation of surfaces has been employed successfully to localize and clock the formation of short-pulse
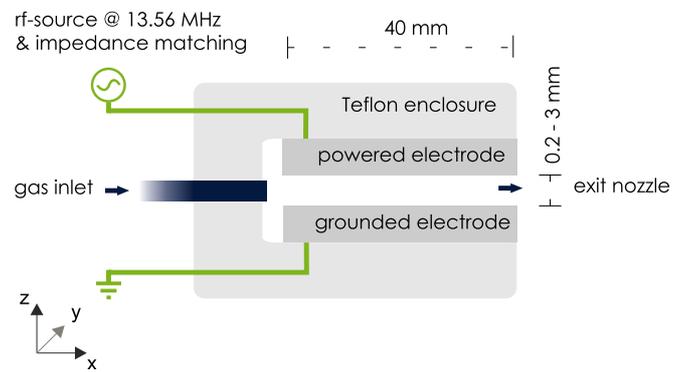

Figure 1. Scheme of the micro-plasma jet discharge.

plasmas in corona-streamer discharges [22]. It is not obvious *a priori* which of the possibly relevant quantities, namely, instantaneous intensity, power, pulse energy and fluence play a dominant role in setting the threshold level and thereby, the optimum experimental conditions. It is likely that several of these factors play a role, thus leading to two separate thresholds, one for peak intensity and one for total energy. It is interesting to note that mechanisms similar to those of laser-surface interaction probably play a role in the glow-to-arc-transition as well.

To the best of our knowledge, there are no reports on 'pump–probe' experiments using a single laser, nor two tightly synchronized lasers, generating a pump and a probe pulse for the establishment of a special state and its subsequent diagnostics, respectively, in the field of micro-plasmas. The evolution of an event can be monitored over several pulses using a variable delay between excitation and read-out pulse. This approach is an adaptation of the well-known ultrafast spectroscopy, notably in the laser-surface interaction at extreme laser powers [19]. It has yielded a wealth of most interesting physics information for transient phenomena. In our case, a custom designed fiber laser system is a unique and new approach to realize laser-assisted pump–probe experiments in micro-plasmas.

2. The atmospheric pressure micro-plasma jet

In this work the techniques of broadband absorption spectroscopy and laser-assisted plasma breakdown are applied to a typical α-mode micro-plasma discharge that is already well characterized concerning its operational range as well as its relevant plasma parameters [25, 26].

The atmospheric pressure micro-plasma jet is a capacitively coupled, non-thermal glow-discharge at high pressures. The design concept of this discharge is based on the plasma jet introduced by Selwyn co-workers in 1998 [27] and advanced by Schulz-von der Gathen *et al* [28]. Feed gas flows between two closely spaced stainless steel electrodes driven at 13.56 MHz radio-frequency in a parallel plate configuration (figure 1). Electrodes and plasma volume are enclosed by quartz windows, giving direct optical access to the discharge. The jet is operated in helium at various flow rates from 200 sccm to 5 slm. The electric field between the electrodes

causes a breakdown in the gas and produces a plasma with electron temperatures and densities of about 1 to 2 eV and 10^{10} cm^{-3}, respectively [31, 32]. Atoms and molecules in the feed gas become excited, dissociated or ionized by electron impacts. Since the electrons are not in thermal equilibrium with the ions and neutrals, the gas temperature remains a few tens of K above room temperature [33]. The distance between the two windows is fixed to 1 mm while the electrode gap size is variable between 0.2 and 3 mm. In all here presented configurations the discharge operates as a typical α-mode rf glow discharge.

3. Fiber laser setup

The fiber laser setup that was custom developed for this application is illustrated in figure 3. The laser system comprises of a mode-locked fiber oscillator, operating in the all-normal dispersion mode, and seeding a multi-stage fiber amplifier. A fiber stretcher is used to implement chirped-pulse amplification. The system is all-fiber, with an architecture based that of [29]. Prior to the final stage, the fiber path bifurcates into two, one seeding the power amplifier, which is described in detail in [30], and another seeding a highly nonlinear PCF for supercontinuum generation. Supercontinuum generation without pulse compression requires high pulse energies, so the repetition rate of the pulses is reduced to 50 kHz in two steps to further increase the pulse energies during amplification while maintaining reasonably low average power levels.

The oscillator comprises about 6 m of standard single-mode fiber for 1 μm wavelength (core diameter of 6.2 μm, NA of 0.14) and Yb-doped gain fiber (core diameter of 6.2 μm, NA of 0.14, $\sim$500 dB m^{-1} absorption at 976 nm). The length of the oscillator cavity defines the output pulse frequency of the laser in the mode-lock operation. The gain fiber is pumped in-core by a telecom-style 976 nm fiber-coupled laser diode with a maximum output power of 600 mW. Fast saturable absorption required for mode-locking is implemented via nonlinear polarization evolution. An output power of 14 mW at 27.12 MHz repetition frequency (set to exactly the second harmonic of 13.56 MHz) is obtained directly through a 10% output coupler after the gain fiber. The power from the seed laser is sufficient to suppress amplified spontaneous emission (ASE) generation in the subsequent amplifying stages.

Following another fiber coupler, around 90% of the output power from the oscillator traverses 500 m of single-mode fiber to stretch the pulses. The stretching is necessary to reduce the peak power of the pulses and thus to minimize the nonlinear effects imposed on the pulses in the following stages. The remaining 10% of the beam is used for diagnostics.

The stretched pulses are amplified and then reduced in repetition rate through acousto-optic modulators (AOMs) to achieve the desired pulse energy in two steps. Amplifier stages consist of 1 m long Yb-doped fiber (of the same type as in the oscillator). 5% of the second AOM output is split off for diagnostics and the rest seeds the third amplifier with 35 cm of Yb-doped fiber. The beam is split where 20% is used to seed the power amplifier and 80% is coupled into the 2 m of PCF

for supercontinuum generation. We used a 976 nm diode with 8 W of maximum power for the power amplifier. The average output power of the power amplifier is around 1.1 W obtained at pump power of 6 W, limited by the onset of nonlinear effects. At a final repetition frequency of 50 kHz, this corresponds to 22 μJ, which is among the highest obtained from a picosecond fiber amplifier. The pulse length of the supercontinuum pulses is about 300 ps with about 166 nJ pulse energy and an average beam power of 8.3 mW.

4. Absorption spectroscopy with supercontinuum radiation

This section provides an overview of the results obtained from broadband absorption spectroscopy on helium and argon metastable transitions using the supercontinuum laser source. The aim is the qualification of this system as a reliable light source for absorption spectroscopic measurements. The metastable transitions have been chosen due to their high oscillator strength, their high density in the discharge, and because these species have turned out to be important for the understanding of energy transport in micro-plasmas as they constitute an important reservoir of potential energy. They seem to influence strongly the dynamics and the stability of the discharges, i.e. they play an important role in transient phenomena. These are in particular the evolution of the discharge in the ignition phase, the γ-transition and the transition into the arc regime.

4.1. Spectroscopic setup

The experimental setup for BBAS measurements is shown in figure 2. The supercontinuum beam from the fiber laser is focused into the discharge where part of the beam is absorbed by diverse plasma species that offer transitions in the range of the supercontinuum spectrum. The transmitted beam is guided on the entrance slit of a spectrometer with 75 cm focal length, which is equipped with a 1200 lines mm^{-1} grating and images the signal to an InGaAs photo diode array. The effective resolution of the system is less than 50 pm. Due to the high spectral intensity of the supercontinuum, the slit opening can be as small as a few μm.

4.2. Spectroscopic results

The emission spectrum of the laser is presented in figure 4. It ranges from roughly 700 to 1700 nm with an intensity profile ranging over about three orders of magnitude. Compared with other light sources, such as incandescent lamps or LEDs, the spectral intensity in the mentioned region is at least an order of magnitude higher, in parts several orders of magnitude, resulting in significantly better signal-to-noise ratios since the opening slit of the spectrometer has to be opened just a few μm. Furthermore, due to the strongly directed beam, the laser radiation offers far better properties regarding focusing alignment of the optical path.

Concerning the time stability of the supercontinuum spectrum, two influences have to be considered. Since the
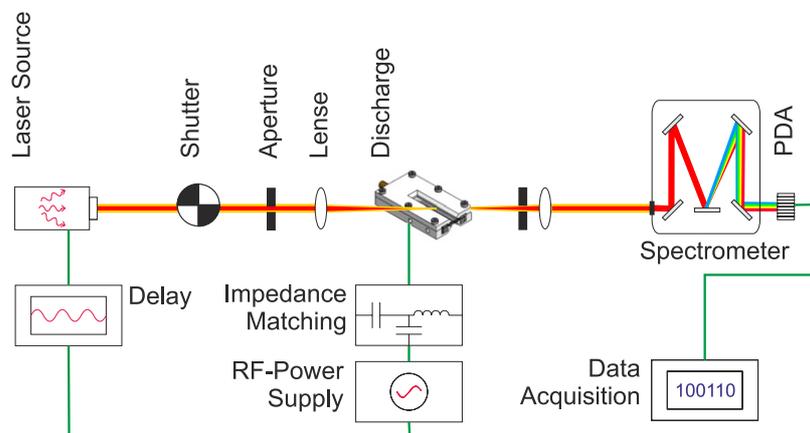
Figure 2. Experimental setup for broad-band absorption measurements with supercontinuum or LED light source.
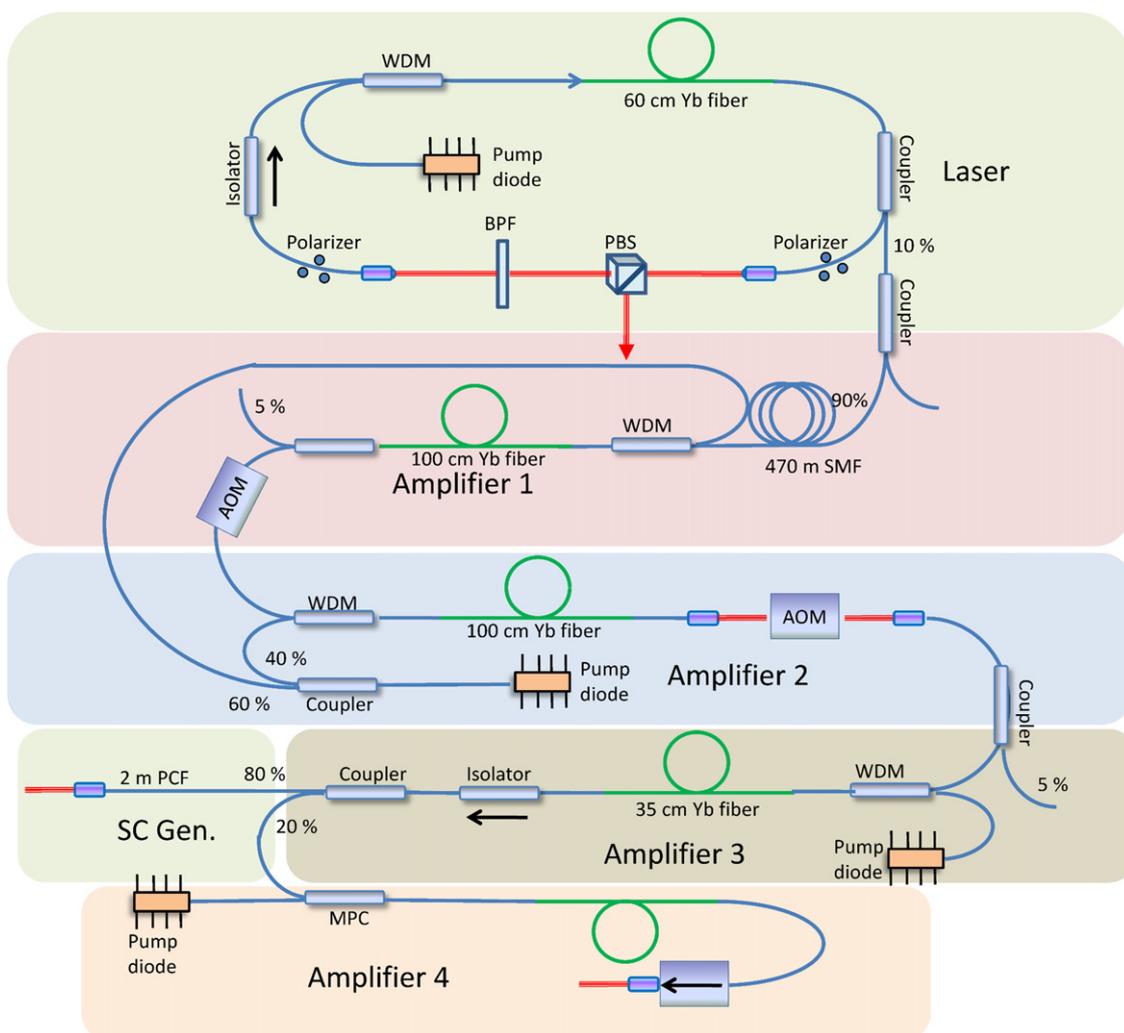

Figure 3. Fibre laser setup for supercontinuum and high-power pulse generation. WDM = wavelength-division multiplexing, PCF = photonic crystal fiber, MPC = multiport pump signal combiner.

broad spectral range is a result of strong nonlinear processes inside the fiber medium, the spectral profile is very sensitive to variations of the power. This effect is compensated by choosing the integration time of the detection system to average over several thousands of pulses, therewith obtaining a stable profile. A second strong impact is given by thermal effects

affecting the spectrum on timescales of several minutes. The high powers necessary to trigger the nonlinear effects probably lead to a warming-up of the SMF-PCF splice point and therewith small changes in the supercontinuum. As a result, an absorption spectroscopic measurement for a single parameter, containing also the measurements of the reference spectrum,
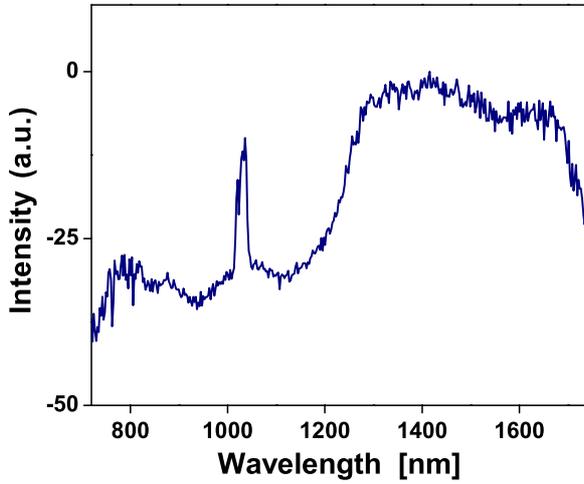
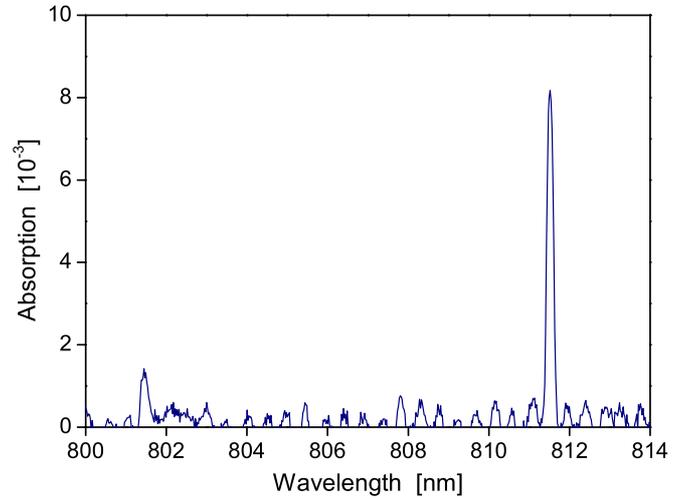**Figure 4.** Spectral profile of the supercontinuum beam (logarithmic scale).

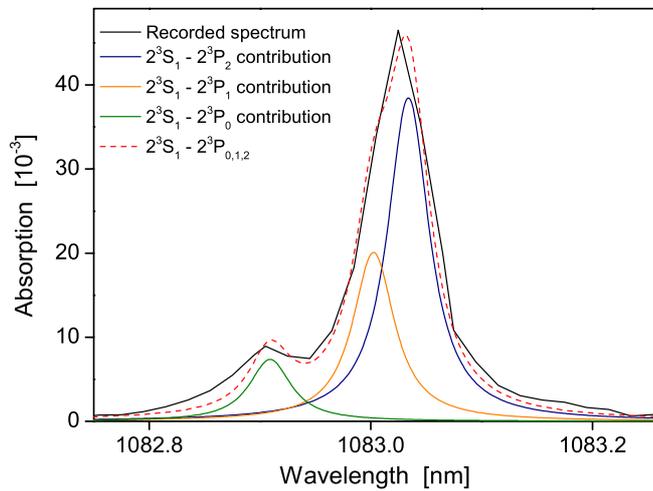**Figure 5.** Absorption spectrum around the He^m $2^3S_1 \rightarrow 2^3P_J^0$ ($J = 0, 1, 2$) transitions at 1083 nm (black line). Recorded with a spectrometer featuring 75 cm focal length, a 1200 lines per mm grating and few μm slit opening, together with a photo diode array as detector. Also displayed are three Voigt functions, representing the respective transitions from the He^m 2^3S_1 level. The functions have been modelled with the results obtained by TDLAS measurements (line width and position) and show perfect agreement with the BBAS measurements.

has to be preformed in a time of about 1 min, which is a compromise between the two described effects. In this case, a detection threshold in the order of 10^{-4} in the absorption can be achieved. This is a far better result than we obtained using LEDs or incandescent lamps.

A typical absorption spectrum around the He^m $2^3S_1 \rightarrow 2^3P_J^0$ ($J = 0, 1, 2$) transitions at 1083 nm is shown in figure 5 (black line). It was recorded with the spectrometer described above and spectrum is already corrected for the instrumental broadening of the optical instruments and the entrance slit of the spectrometer. Also displayed are three Voigt functions, representing the respective transitions from the He^m 2^3S_1 level. The functions have been modeled with the results obtained by TDLAS measurements which have been discussed in detail in a previous publication and are not shown here [25]. Although the spectral resolution of BBAS is limited, compared with the

Figure 6. Absorption spectrum around the argon transitions at 801.5 and 811.5 nm.

possibilities of tunable diode lasers, these results show that sufficient information can be obtained to retrace the line profile and obtain a perfect agreement with TDLAS measurements.

The detection limit of BBAS using supercontinuum radiation on the given discharge geometry is at least in the order of 10^{-3} as shown by figure 6, that presents two argon transitions at 801.5 and 811.5 nm. The sensitivity depends critically on the extend of the periodic noise pattern visible in this graph. This noise pattern is the consequence of an etalon effect between the glass plates that confine the discharge channel of the micro-plasma jet. These limitations can be suppressed by operating the jet discharge without the glass windows in an airtight chamber filled with the working gas, extending the detection limit further.

After showing the effectiveness of BBAS for the application on micro-plasma, the investigation of transient phenomena requires a well-synchronized connection to the trigger that transfers the plasma into another mode. This is demonstrated in the following section.

5. Laser-assisted plasma breakdown and phase-resolved absorption

The RF voltage thresholds for plasma ignition and collapse in the micro-plasma do not overlap, but show a certain hysteresis, where the discharge ignites at higher voltages than it collapses when decreasing the electrode voltage. This hysteresis effect is visualized in figure 7. The hysteresis length depends on a variety of factors, such as the electrode gap width, the gas mixture as well as the electrical characteristics of the matching network, but it can account for up to 25% of the overall voltage.

This hysteresis effect can be utilized to trigger the discharge's ignition externally by superposing high-power laser beams with the electric field between the electrodes or using the laser beam to release free electrons from the electrode surfaces, while the RF voltage is between ignition and collapse value of the discharge. The first way requires extremely high peak powers and a strong focus point at an arbitrary position in the jet volume. However, the substantial energy
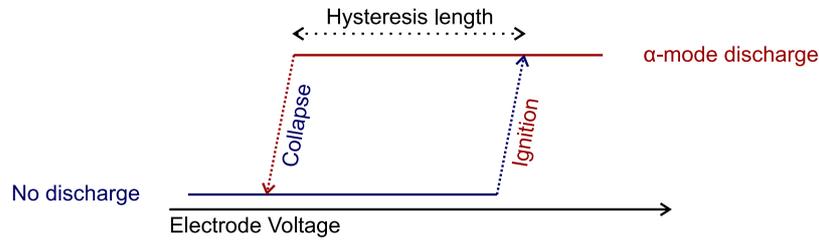
J. Phys. D: Appl. Phys. **45** (2012) 245202

B Niermann *et al*

Figure 7. Discharge ignition and collapse hysteresis of the micro-plasma jet.
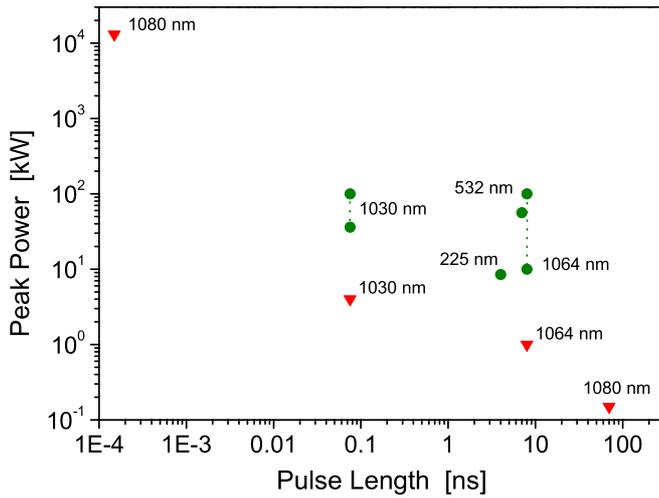

Figure 8. Parameter diagram for successful (green circles) and unsuccessful (red triangles) breakdown attempts in dependance of wavelength, pulse length and peak powers. Right: Sketch of the experimental setup for laser assisted plasma breakdown.
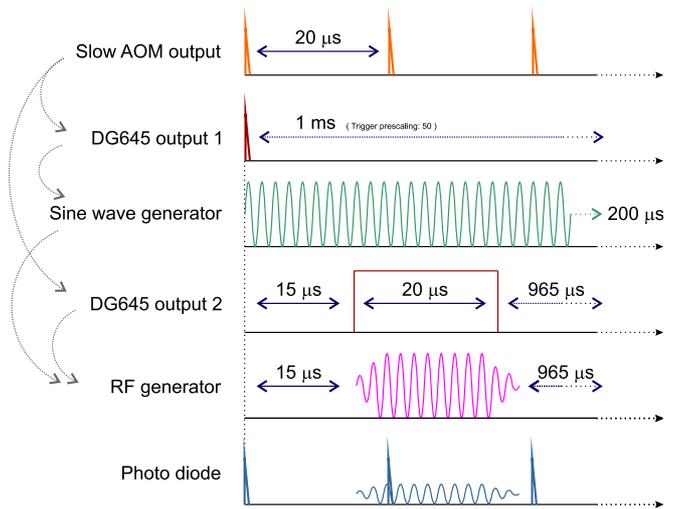

Figure 9. Trigger sequence for phase locked operation of fibre laser and RF generator. AOM = acousto-optic modulator, DG645 = delay generator.

loss that the high-power beam experiences when passing the glass windows of the jet usually leads to the destruction of the material and the containment of the working gas atmosphere is lost. The second way requires significantly less peak powers, but makes it necessary to have a tight focus on the surface of the electrode that faces the plasma volume. A possible explanation for plasma ignition is the release of free electrons from the surface by the intense laser field, that can afterwards be utilized as seed electrons for plasma breakdown. Another reason could be the release of atomic or molecular species with low ionization thresholds that open a low energy path for seed electron generation. The critical point in the ignition process is the creation of an avalanche and the release of secondary electrons by ions. Once the discharge is ignited, the plasma remains in a stable α-mode as long as the electrode voltage is above the collapse threshold.

In order to reveal the physical mechanism of plasma ignition by strong laser fields, we utilized a variety of lasers that differ in wavelength, pulse length, and peak power. Figure 8 gives on overview about successful (green circles) and unsuccessful (red triangles) breakdown attempts in dependence of the three mentioned parameters. The results suggest that the wavelength (photon energy) is not a critical parameter and shows no visible effect compared with the peak power and the pulse length. However, even much higher peak powers may not be sufficient when the pulse length is very short. This was shown by measurements using pulses with

a peak power of about 13 MW, but a pulse length of just 150 fs, obtained from another fiber laser [34], which failed to ignite the plasma. On the other hand a long interaction time with 70 ns pulses was not successful when the power density was too low to have an effect on the metal surface. The minimum necessary pulse length for plasma ignition that was observed in our experiments was 75 ps, with peak powers in the order of 10 kW. As described before, the critical point for establishing a self-supporting plasma is the formation of an avalanche. Therefore, the interaction time of electric field and the discharge must be long enough to allow surface and metastable driven processes to evolve and therewith maintain a continuous discharge.

One application of this external plasma ignition is the opportunity of highly time-resolved diagnostics of the ignition phase. Furthermore, since the RF phase can be synchronized with the laser frequency, the laser is able to set the ignition point with a precision of less than one nanosecond and at a selectable phase of the RF cycle. For this purpose, it is mandatory to synchronize the laser pulses with the RF generator. The necessary setup is visualized in figure 9.

The output power of the high-power amplifier is about 1.1 W distributed on 50 kHz pulses with about 300 ps pulse length. Thus, each pulse carries about 22 μJ of energy. A small fraction of the laser pulses is extracted behind the slow AOM and is used as a trigger signal for a delay generator. The delay generator provides a 1 kHz trigger for an arbitrary
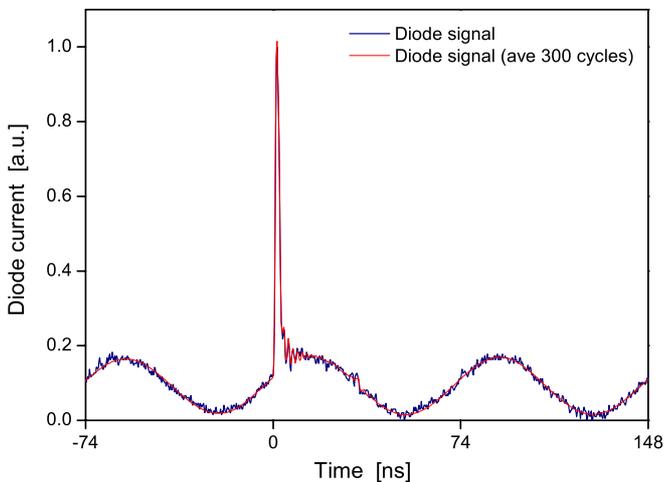
J. Phys. D: Appl. Phys. **45** (2012) 245202

B Niermann *et al*

Figure 10. Current signal of a photo diode placed behind the discharge. The current shows the laser pulses as well as the RF signal that is phase locked to the laser.

waveform generator that produces a 13.56 MHz sinus burst with a length of 50 μs. This sinus signal is a reference for the RF generator that matches the phase of its 13.56 MHz output to the phase of the waveform generator. As a result, the RF output is synchronous to the laser pulses. The phase delay can easily be adjusted via the delay generator. To make sure that the discharge is ignited by a certain laser pulse, the delay generator provides a second output that is used for turning the discharge on and off. As a result, the RF generator is activated below the threshold about 5 μs before the laser strikes. After the discharge ignites, the RF generator runs for 15 μs before it shuts the system down. The phase relation between laser pulses and RF can be monitored by a photo diode placed behind the discharge. Both laser and RF induce a current in the diode that overlap and show the laser pulse within the 13.56 MHz sinus burst with sub-nanosecond precision.

Once the discharge is ignited, the plasma remains in a stable α-mode as long as the electrode voltage is above the collapse threshold. One application of this external plasma ignition is the opportunity of highly time-resolved diagnostics of the ignition phase. Usually the rise of excited species after the ignition is slightly affected by the not instantaneously rising power level of the RF generator. With the help of the high-power laser beam, it is possible to activate the RF generator below the ignition threshold and activate the discharge once the RF power is stable. Furthermore, since the RF phase can be synchronized with the laser frequency, the laser is able to set the ignition point with a precision of less than 100 ps and at a selectable phase of the RF cycle. Figure 10 shows the current signal of a photo diode placed behind the discharge. The current shows the laser pulses as well as the RF signal that is phase locked to the laser. Utilizing this technique, a sub-nanosecond phase-resolved spectroscopic analysis of the ignition process can be realized.

6. Summary

BBAS measurements using fiber laser generated supercontinuum spectra provide a way for absorption spectroscopic mea-surement over a broad spectral range with detection thresholds down to 10^{-4} in the absorption signal. To a certain extent, the technique was therefore proven to provide competitive results to TDLAS approaches if observing species that have suffi-ciently high densities in the discharge and transitions with a sufficiently high oscillator strength. The much superior sta-bility and spectral brightness of the supercontinuum spectrum certainly gives rise to applications that were not accessible by past attempts with other broadband sources such as LEDs or incandescent lamps.

The hysteresis of discharge ignition and collapse together with the possibility of phase-locked laser-assisted breakdown offers a tool for highly time-resolved studies of the plasma breakdown process.

Acknowledgments

References

[1] Sadeghi N 2004 *J. Plasma Fusion Res.* **80** 767
[2] Bear D S and Hanson R K 1992 *J. Quant. Spectrosc. Radiat. Transfer* **47** 455
[3] Becker K H, Schoenbach K H and Eden J G 2006 *J. Phys. D: Appl. Phys.* **39** R55
[4] Belostotskiy S, Khandelwal R, Wang Q, Donnelly V M, Economou D J and Sadeghi N 2008 *Appl. Phys. Lett.* **92** 221507
[5] Belostotskiy S, Donnelly V M, Economou D J and Sadeghi N 2009 *IEEE Trans. Plasma Sci.* **37** 852
[6] Belostotskiy S, Ouk T, Donnelly V M, Economou D J and Sadeghi N 2010 *J. Appl. Phys.* **107** 053305
[7] Roepcke J, Mechold L, Duten X and Rousseau A 2001 *J. Phys. D: Appl Phys.* **34** 2336
[8] Penache C, Miclea M, Braeuning-Demian A, Hohn O, Schoessler S, Jahnke T, Niemax K and Schmidt-Boecking H 2002 *Plasma Sources Sci. Technol.* **11** 47
[9] Miclea M, Kunze K, Heitmann U, Florek S, Franzke J and Niemax K 2005 *J. Phys. D: Appl. Phys.* **38** 1709
[10] Cunge G, Vempaire D, Touzeau M and Sadeghi N 2004 *Appl. Phys. Lett.* **91** 231503
[11] Gherman T, Eslami E, Romanini D, Kassi S, Vial J C and Sadeghi N 2004 *J. Phys. D: Appl. Phys.* **37** 2408
[12] Booth J P, Cunge G, Neuilly F and Sadeghi N 1998 *Plasma Sources Sci. Technol.* **7** 423
[13] Kogelschatz M, Cunge G, and Sadeghi N 2004 *J. Phys. D: Appl. Phys.* **37** 1954
[14] Ranka J K, Windeler R S and Stentz A J 2000 Visible continuum generation in air-silica microstructure optical fibers with anomalous dispersion at 800 nm *Opt. Lett.* **25** 25–7
[15] Knight J C, Birks T, Russell P and Atkin D 1996 All-silica single-mode optical fiber with photonic crystal cladding *Opt. Lett.* **21** 1547
[16] Herrmann J, Bruneau S and Sentis M 2004 *Thin Solid Films* **453** 377

[17] Margetic V, Pakulev A, Stockhaus A, Bolshov M, Niemax K and Hergenroeder R 2000 *Spectrochim. Acta B* **55** 1771

[18] Mizunami T, Kizaki N and Nagaiwa K 2007 *Japan. J. Appl. Phys.* **46** 5450

[19] von der Linde D and Schueler H 1996 *J. Opt. Soc. Am.* B **13** 216

[20] Mitchell A, Scheller G and Gottscho A 1989 *Phys. Rev. A* **40** 5199

[21] Debontride H, Derouard J, Edel P, Romestain R, Sadeghi N and Boeuf J 1989 *Phys. Rev.* A **40** 5208

[22] Luque A, Ratushnaya V and Ebert U 2008 *J. Phys. D: Appl. Phys.* **41** 234005

[23] Berden G, Peters R and Mejer G 2000 *Int. Rev. Phys. Chem.* **19** 565

[24] Wang C and Srivastava N 2010 *Eur. Phys. J. D* **60** 465

[25] Niermann B, Böke M, Sadeghi N and Winter J 2010 *Eur. Phys. J. D* **60** 489–95

[26] Niermann B, Kanitz A, Böke M and Winter J 2011 *J. Phys. D: Appl. Phys.* **44** 325201

[27] Schütze A, Jeong J Y, Babayan S E, Park J, Selwyn G S and Hicks R F 1998 *IEEE Trans. Plasma Sci.* **26** 1685

[28] Schulz-von der Gathen V, Buck V, Gans T, Knake N, Niemi K, Reuter S, Schaper L and Winter J 2007 *Contrib. Plasma Phys.* **47** 510–19

[29] Ilday F Ö, Lim H, Buckley J and Wise F W 2003 *Opt. Lett.* **28** 1362

[30] Mukhopadhyay P K, Özgören K, Budunoglu I L and Ilday F Ö, 2009 *IEEE J. Sel. Top. Quant.* **15** 145

[31] Schaper L, Reuter S, Waskoenig J, Niemi K, Schulz-von der Gathen V and Gans T 2009 *J. Phys. Conf.* **162** 012013

[32] Waskoenig J, Niemi K, Knake N, Graham L M, Reuter S, Schulz-von der Gathen V and Gans T 2010 *Pure Appl. Chem.* **82** 1209

[33] Knake N, Reuter S, Niemi K, Schulz-von der Gathen V and Winter Jörg 2008 *J. Phys. D: Appl. Phys.* **41** 194006

[34] Kalaycoglu H, Oktem B, Senel C, Paltani P P and Ilday F Ö 2010 *Opt. Lett.* **35** 959